Effect of Donor-Acceptor Orientation on Ultrafast Photoinduced Electron Transfer and Dark Charge Recombination in Porphyrin-Quinone Molecules

Yoshiteru Sakata,† Hirohito Tsue,† Michael P. O'Neil,‡ Gary P. Wiederrecht,‡ and Michael R. Wasielewski*,‡

Contribution from The Institute of Scientific and Industrial Research, Osaka University, Mihoga-oka, Ibaraki, Osaka 567, Japan, and Chemistry Division, Argonne National Laboratory, Argonne, Illinois 60439

Received April 14, 1994®

Abstract: A series of four zinc porphyrin-spacer-benzoquinone molecules were studied in which the spacer is either spiro[4.4]nonane or *trans*-decalin. The benzoquinone is attached to the porphyrin at two fixed distances each possessing two fixed orientations of the porphyrin relative to the quinone. The rate constants for photoinduced electron transfer from the lowest excited singlet state of the porphyrin to the quinone to form the Zn porphyrin$^+$-quinone$^-$ ion pair and the subsequent dark charge recombination reaction were measured as a function of solvent polarity. The observed orientation dependent differences in rate constants for these two reactions can be attributed to orientation dependent changes in electronic coupling alone, because the Franck-Condon factors for electron transfer are similar for each molecule. The rate constant data suggest that the donor-acceptor orientation effects observed are due to variations in the sum of the direct, through-space interaction between the donor and acceptor and the indirect, through-solvent term. The rate constant data and AM1 molecular orbital calculations support the idea that the indirect interaction of the donor with the acceptor through the covalent bonds of the spacer is approximately constant for the spacers employed in this study.

Introduction

In recent years significant research has been directed toward understanding the dynamics of electron transfer in both protein and molecular systems. Photoinduced electron transfer reactions are of special interest because photosynthesis provides us with the prime example of how a carefully designed array of electron donors and acceptors can be used to capture and store photon energy.[1-3] In photosynthetic proteins a sequence of highly efficient electron transfer reactions occur between chlorophyll donors and quinone acceptors whose mutual distances and orientations are restricted by the surrounding protein.[4] Our understanding of these reactions has been aided greatly by studies of electron transfer in covalently-linked donor-acceptor systems. The principal reason for studying covalent donor-acceptor molecules is to eliminate diffusion as a source of kinetic complexity, thus making it possible to study reactions with rate constants that may be substantially faster than diffusion. Within this regime previous studies of photoinduced electron transfer reactions have focused largely on the free energy[5-8] and distance dependence[9-14] of these reactions. The same problems have been studied in great detail for charge shift reactions.[15,16] A few studies concerning the dependence of photoinduced electron transfer rates on the mutual orientation of the donor and the acceptor have also appeared.[17-22] The relatively small number of such studies is due to the synthetic challenges that arise when a series of very specific molecular distances and orientations are required.

Our work focuses on singlet state electron transfer reactions because these processes are generally very rapid and result in the greatest overall storage of photon energy in the ion pair products. In this paper we present ultrafast kinetic measurements of the rate constants for photoinduced charge separation and subsequent dark charge recombination as a function of molecular geometry for the series of porphyrin-spacer-quinone molecule SP-H, SP-V, TD-H, and TD-V, illustrated in Chart 1. Two types of rigid hydrocarbon spacer are employed to maintain a benzoquinone electron acceptor at a fixed distance and orientation relative to the adjacent zinc porphyrin electron donor. Rotation of the spacer-quinone unit relative to the porphyrin is strongly restricted by the steric effects of the methyl groups adjacent to the porphyrin

† Osaka University.
‡ Argonne National Laboratory.
® Abstract published in *Advance ACS Abstracts,* July 1, 1994.

(1) Wasielewski, M. R. *Chem. Rev.* **1992**, *92*, 435.
(2) Wasielewski, M. R. *Photoinduced Electron Transfer, Part A*; Fox, M. A., Chanon, M., Eds.; Elsevier: Amsterdam, 1988; Chapter 1.4.
(3) Connolly, J. S.; Bolton, J. R. *Photoinduced Electron Transfer, Part D*; Fox, M. A., Chanon, M., Eds.; Elsevier: Amsterdam, 1988; Chapter 6.2.
(4) Deisenhofer, J.; Epp, O.; Miki, K.; Huber, R.; Michel, H. *J. Mol. Biol.* **1984**, *180*, 385.
(5) Wasielewski, M. R.; Niemczyk, M. P.; Svec, W. A.; Pewitt, E. B. *J. Am. Chem. Soc.* **1985**, *107*, 1080.
(6) Joran, A. R.; Leland, B. A.; Felker, P. M.; Zewail, A. H.; Hopfield, J. J.; Dervan, P. B. *Nature* **1987**, *327*, 508.
(7) Wasielewski, M. R.; Johnson, D. G.; Svec, W. A. In *Supramolecular Photochemistry*; Balzani, V., Ed.; D. Reidel: Amsterdam, 1987; p 255 ff.
(8) Gaines, G. L.; O'Neil, M. P.; Svec, W. A.; Niemczyk, M. P.; Wasielewski, M. R. *J. Am. Chem. Soc.* **1991**, *113*, 719.
(9) Joran, A. R.; Leland, B. A.; Geller, G. G.; Hopfield, J. J.; Dervan, P. B. *J. Am. Chem. Soc.* **1984**, *106*, 6090.
(10) Wasielewski, M. R.; Niemczyk, M. P. In *Porphyrins—Excited States and Dynamics*; Gouterman, M., Rentzepis, P. M., Straub, K. D., Eds.; ACS Symposium Series No. 321; American Chemical Society: Washington, DC, 1986; p 154 ff.
(11) Penfield, K. W.; Miller, J. R.; Paddon-Row, M. N.; Cotsaris, E.; Oliver, A. M.; Hush, N. S. *J. Am. Chem. Soc.* **1987**, *109*, 5061.
(12) Antolovich, M.; Keyte, P. J.; Oliver, A. M.; Paddon-Row, M. N.; Kroon, J.; Verhoeven, J.; Jonker, S. A.; Warman, J. M. *J. Phys. Chem.* **1990**, *95*, 1933.
(13) Knapp, S.; Murali Dhar, T. G.; Albaneze, J.; Gentemann, S.; Potenza, J. A.; Holten, D.; Shugar, H. J. *J. Am. Chem. Soc.* **1991**, *113*, 4010.
(14) Warman, J. A.; Smit, K. J.; de Haas, M. P.; Jonker, S. A.; Paddon-Row, M. N.; Oliver, A. M.; Kroon, J.; Oevering, H.; Verhoeven, J. W. *J. Phys. Chem.* **1991**, *95*, 1979.
(15) Miller, J. *New J. Chem.* **1987**, *11*, 83.
(16) Closs, G. L.; Miller, J. R. *Science*, **1988**, *240*, 440.
(17) Cave, R.; Marcus, R.; Siders, P. *J. Phys. Chem.* **1986**, *90*, 1436.
(18) Oliver, A. M.; Craig, D. C.; Paddon-Row, M. N.; Kroon, J.; Verhoeven, J. W. *Chem. Phys. Lett.* **1988**, *150*, 366.
(19) Oevering, H.; Verhoeven, J. W.; Paddon-Row, M. N.; Warman, J. M. *Tetrahedron* **1989**, *45*, 4751.
(20) Wasielewski, M. R.; Niemczyk, M. P.; Johnson, D. G.; Svec, W. A.; Minsek, D. W. *Tetrahedron* **1989**, *45*, 4785.
(21) Wasielewski, M. R.; Johnson, D. G.; Niemczyk, M. P.; Gaines, G. L.; O'Neil, M. P.; Svec, W. A. *J. Am. Chem. Soc.* **1990**, *112*, 6482.
(22) Helms, A.; Heiler, D.; McLendon, G. L. *J. Am. Chem. Soc.* **1991**, *113*, 4325.

0002-7863/94/1516-6904$04.50/0

Chart 1

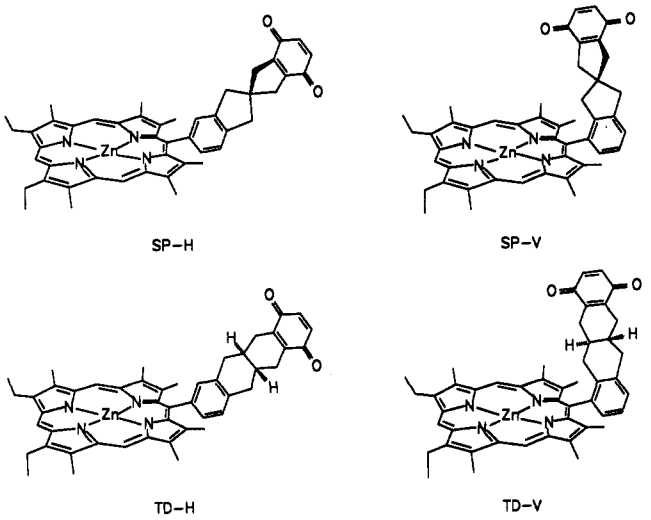

meso position to which the spacer is attached.[21] The spiro[4.4]-nonane spacer (SP) and the *trans*-decalin (TD) spacer provide very similar distances and equal numbers of saturated bonds between the π systems of the porphyrin and the quinone, while providing porphyrin–quinone orientations that differ by 90°. In addition, the spacers are attached to the porphyrin using two different positions of their corresponding benzene rings. Thus, two of these molecules, SP-V and TD-V, possess significantly shorter porphyrin–quinone distances than do SP-H and TD-H. The center-to-center (edge-to-edge) distances between the porphyrin and the quinone in these four molecules are as follows: SP-H, 12.5 Å (8.2 Å); TD-H, 12.9 Å (8.6 Å); SP-V, 9.0 Å (6.4 Å); TD-V, 9.3 Å (6.3 Å).[25]

We have chosen porphyrin–quinone systems to carry out this study for two principal reasons. First, porphyrin–quinone molecules provide a system in which electron transfer occurs with energetic requirements similar to those of photosynthetic systems. Second, there exists a large data base on porphyrin–quinone molecules to compare with the data obtained on the fixed-distance, fixed-orientation systems reported here.[1-3] Preliminary results pertaining to the photoinduced charge separation rate constants for the corresponding molecules possessing a free-base porphyrin electron donor show that the rates of charge separation depend strongly on the mutual orientation of the porphyrin and quinone.[23,24]

Experimental Section

The syntheses of the free-base porphyrin–quinone molecules have been reported previously.[23,24] Insertion of Zn into the porphyrin was accomplished with zinc acetate in MeOH/$CHCl_3$ using a procedure described earlier.[21] Samples for transient absorption measurements were 2×10^{-4} M. The solvents utilized were HPLC grade toluene (TOL), tetrahydrofuran (THF), and *N,N*-dimethylformamide (DMF). TOL and DMF were re-distilled and stored over Linde 3A molecular sieves, while THF was freshly distilled from lithium aluminum hydride before use. UV–visible absorption spectra were taken on a Shimadzu UV-160.

The laser system utilized for the pump-probe experiments consists of a synchronously-pumped femtosecond dye laser and regenerative amplifier. The CW mode-locked Nd-YAG pump laser is based on a Spectra-Physics 3460 CW laser. The mode-locker is made by NEOS and operates at 41 MHz. The laser typically produces 10 W of CW mode-locked power. A 5 mm KTP crystal (CSK) is utilized to produce 1.2 W of 532 nm light.

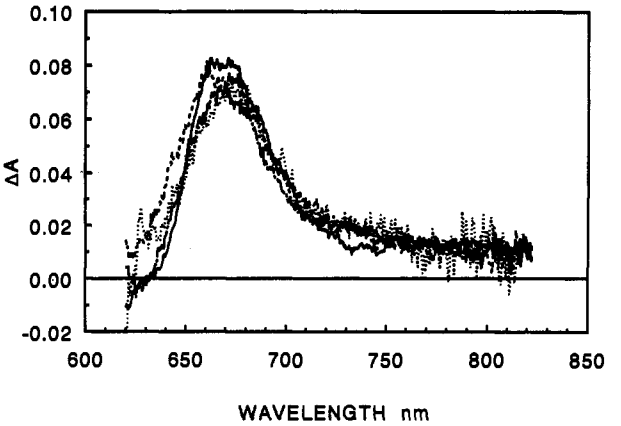

Figure 1. Transient absorption spectra of TD-H (—), SP-H (- - -), SP-V (– • –), and TD-V (•••) in THF at 100, 60, 40, and 20 ps, respectively, following a 190 fs, 585 nm laser flash.

A linear dye laser possessing a rhodamine 6 G gain jet, a DQOCl saturable absorber jet, and two dispersion compensating prisms produces 180 fs pulses at an 82 MHz repetition rate with approximately 100 mW of average power. The regenerative amplifier is nearly identical in design to that published by Postlewaite et al.[26] and produces 1.2 mJ pulses at 1064 nm with a 1 kHz repetition rate. A 5 mm long KTP crystal is utilized to produce 600 μJ pulses at 532 nm. The 532 nm light from the regenerative amplifier is used to pump a three-stage dye amplifier (rhodamine B) to produce 20 μJ, 190 fs, 585 nm pulses at a 1 kHz repetition rate. This beam is subsequently sent through a 80/20 beam splitter. The smaller portion is focused with a 15 cm focal length lens into a 1.0 cm flowing cell of $CCl_4/CHCl_3$ (3/1, v/v) to generate a white light continuum that is used as the probe light. The probe beam is divided into reference and measuring beams by a 50/50 beam splitter. The excitation and measuring probe beams are focused with a 15 cm focal length lens and are directed nearly collinearly through the sample, which is stirred in a 1 cm path length cuvette. The arrival of the measuring probe beam relative to the excitation beam is adjusted with a motorized optical delay line. The reference probe beam is directed around the sample. Both probe beams are then focused onto different vertical segments on the slit of an ISA HR-320 monochromator. The monochromator disperses both beams onto the top and bottom halves of the face of an intensified SIT detector which is part of an optical multichannel analyzer (PAR OMA II). Data from the OMA are collected by a personal computer (Gateway 386, 33 MHz). The formation and decay kinetics were fit through a Marquardt–Levenberg least-squares fitting routine.

Results

The fluorescence lifetimes of the free-base molecules corresponding to those investigated here depend strongly on the porphyrin–quinone geometry.[23,24] These changes in fluorescence lifetime were attributed to variations of the charge separation rate constant with donor–acceptor geometry. However, fluorescence lifetime data cannot determine the rate constants for charge recombination because these reactions in most porphyrin–quinone molecules are nonradiative. Moreover, time-correlated single photon counting measurements are intrinsically inaccurate at the high time resolutions needed to determine some of the rate constants for photoinduced charge separation in the molecules studied here. Thus, we have measured the rate constants of electron transfer in these molecules directly by monitoring the appearance and decay of the characteristic absorption band near 670 nm for the Zn octaalkylporphyrin cation radical.[27] This band is narrower and more well-defined than the corresponding band in Zn meso-substituted porphyrins.

Figure 1 shows the transient absorption spectra of each of these molecules in THF following a 190 fs, 585 nm laser pulse.

(23) Sakata, Y.; Nakashima, S.; Goto, Y.; Tatemitsu, H.; Misumi, S.; Asahi, T.; Hagihara, M.; Nishikawa, S.; Okada, T.; Mataga, N. *J. Am. Chem. Soc.* **1989**, *111*, 8979.

(24) Sakata, Y.; Tsue, H.; Goto, Y.; Misumi, S.; Asahi, T.; Nishikawa, S.; Okada, T.; Mataga, N. *Chem. Lett.* **1991**, 1307.

(25) The distances were determined from MM2 energy minimized structures using HyperChem software.

(26) Postlewaite, J. C.; Miers, J. B.; Reiner, C. C.; Dlott, D. D. *IEEE J. Quantum Electron.* **1988**, *24*, 411.

(27) Fajer, J.; Borg, D. C.; Forman, A.; Dolphin, D.; Felton, R. H. *J. Am. Chem. Soc.* **1970**, *92*, 3451.

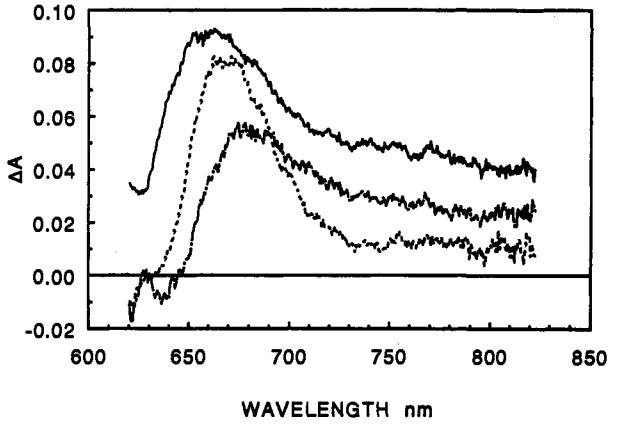

Figure 2. Transient absorption spectra of TD-H in TOL (—), THF (- - -), and DMF (– • –), obtained at 100, 200, and 100 ps, respectively, following a 190 fs, 585 nm laser flash.

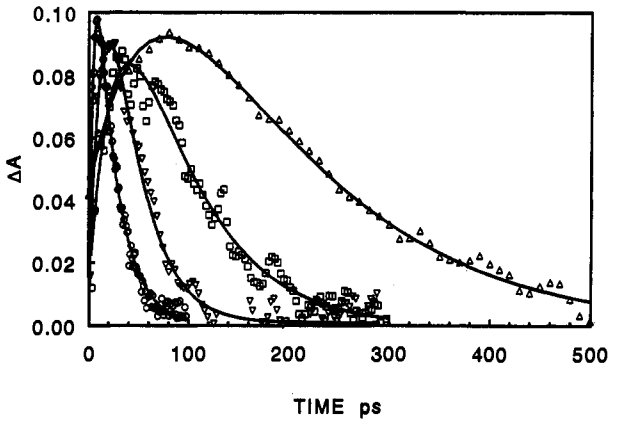

Figure 3. Appearance and decay kinetics at 670 nm for the zinc porphyrin cation radical produced following excitation of TD-H (Δ), SP-H (□), TD-V (∇), and SP-V (○) in THF with 190 fs, 585 nm laser flashes.

Table 1. Rate Constants (s^{-1})

	toluene		THF		DMF	
	k_{cs}	k_{cr}	k_{cs}	k_{cr}	k_{cs}	k_{cr}
SP-V	2.0×10^{11}	1.7×10^{10}	2.6×10^{11}	4.6×10^{10}	5.0×10^{11}	1.8×10^{11}
TD-V	2.9×10^{10}	1.4×10^{9}	3.2×10^{10}	3.6×10^{10}	3.1×10^{11}	5.6×10^{10}
SP-H	5.0×10^{10}	1.0×10^{10}	1.7×10^{10}	1.6×10^{10}	1.2×10^{11}	5.3×10^{10}
TD-H	6.8×10^{10}	5.1×10^{9}	5.0×10^{9}	7.9×10^{9}	5.0×10^{10}	1.2×10^{10}

The cation radical band at 670 nm is similar for each molecule. Figure 2 compares the same spectral region for TD-H in TOL, THF, and DMF. The wavelength of the Zn porphyrin cation radical band shifts slightly redder and broadens as the polarity of the solvent increases. The peak of the cation radical spectrum occurs at 660, 670, and 680 nm in TOL, THF, and DMF, respectively. Similar spectral changes were observed for the remaining three molecules and are not shown. Figure 3 shows the kinetics for the appearance and decay of the zinc porphyrin cation radical at the 670 nm band for all four molecules in THF. The kinetic fits to the data shown in Figure 3 assume a series mechanism ^{1}*PQ → P$^+$Q$^-$ → PQ, where P is the porphyrin and Q is the quinone. The data show that there are large differences in both the formation and decay rates for the radical ion pair intermediate as the distance and geometry of the porphyrin relative to the quinone changes. Figure 4 shows the appearance and decay kinetics of the zinc porphyrin cation radical for TD-H in TOL, THF, and DMF monitored at 670 nm. The fits to the kinetic data directly yield the rate constants for the electron transfer reactions of these molecules. These rate constants are presented in Table 1.

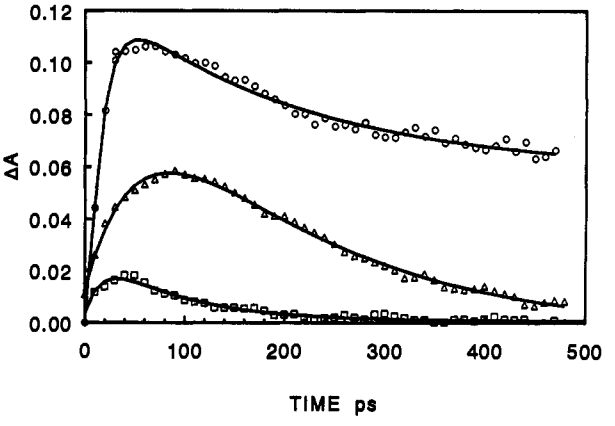

Figure 4. Appearance and decay kinetics at 670 nm for the zinc porphyrin cation radical produced following excitation of TD-H in TOL (○), THF (Δ), and DMF (□) with 190 fs, 585 nm laser flashes.

Discussion

An analysis of the dependence of electron transfer rate constants on the orientation of the electron donor relative to the electron acceptor must include several parameters. In non-adiabatic electron transfer reactions the rate constant, k_{et}, can be expressed as the product of $2\pi/\hbar$ times the square of the electronic coupling matrix element, V, and a Franck–Condon weighted density of states (FCWD), eq 1.[28-30]

$$k_{et} = \frac{2\pi V^2}{\hbar}(\text{FCWD}) \tag{1}$$

where the FCWD, eq 2, depends on the free energy of reaction, ΔG,

$$\text{FCWD} = \left(\frac{1}{4\pi\lambda_s kT}\right)^{1/2} \sum_{m=1}^{\infty} \frac{s^m e^{-s}}{m!} e^{-(\lambda_s \Delta G + m\omega)^2/4\lambda_s kT} \tag{2}$$

λ_s is the solvent reorganization energy, $s = \lambda_V/\hbar\omega$, in which λ_V is the internal reorganization energy, and ω is the frequency of a single internal vibrational mode within the donor–acceptor molecule coupled to the electron transfer reaction. If the solvent is treated as a dielectric continuum using the Born model, Marcus has shown that the solvent reorganization energy, λ_s, can be expressed as eq 3:[31]

$$\lambda_s = e_o^2\left(\frac{1}{2r_1} + \frac{1}{2r_2} - \frac{1}{r_{12}}\right)\left(\frac{1}{\epsilon_o} - \frac{1}{\epsilon_s}\right) \tag{3}$$

where e_o is the electronic charge, r_1 and r_2 are the radii of the charge separated ions, r_{12} is the center-to-center distance between them, ϵ_o is the high frequency dielectric constant of the solvent, often approximated by n^2, where n is the refractive index of the medium, and ϵ_s is the static dielectric constant of the solvent. Equation 3 shows that λ_s depends on the distance between the ions and their sizes.

In polar liquids the energetics of photoinduced electron transfer from the lowest excited singlet state of the zinc porphyrin to the quinone, ΔG_{cs}, can be estimated with reasonable accuracy using the one-electron oxidation, E_{ox}, and reduction, E_{red}, potentials of the donor and acceptor, respectively, and the Coulomb stabiliza-

(28) Hopfield, J. J. *Proc. Natl. Acad. Sci. USA* **1974**, *71*, 3640.
(29) Jortner, J. *J. Chem. Phys.* **1976**, *64*, 4860.
(30) Marcus, R. A. *J. Chem. Phys.* **1984**, *81*, 4494.
(31) Marcus, R. A. *J. Chem. Phys.* **1965**, *43*, 679.

Table 2. Energetics and FCWD for Charge Separation and Recombination

	λ_s (eV)	$-\Delta G_{cs}$ (eV)	$FCWD_{cs}$ (cm)	$-\Delta G_{cr}$ (eV)	$FCWD_{cr}$ (cm)
toluene					
SP-V	0.07	0.32	1.4	1.82	0.00013
TD-V	0.07	0.30	1.7	1.84	0.000089
SP-H	0.09	0.14	0.26	2.00	0.000031
TD-H	0.09	0.13	0.19	2.01	0.000027
THF					
SP-V	0.68	0.83	0.97	1.31	0.64
TD-V	0.70	0.82	0.88	1.32	0.67
SP-H	0.85	0.76	0.30	1.38	0.86
TD-H	0.86	0.76	0.29	1.38	0.88
DMF					
SP-V	0.88	1.05	0.96	1.09	1.03
TD-V	0.93	1.05	0.84	1.09	0.93
SP-H	1.08	1.04	0.45	1.10	0.59
TD-H	1.10	1.04	0.41	1.10	0.54

tion of the ion-pair:

$$\Delta G_{cs} = E_{ox} - E_{red} - \frac{e_o^2}{\epsilon_s r_{12}} - E_s \qquad (4)$$

where E_s is the energy of the lowest excited singlet state of the porphyrin donor determined from the frequency of the (0,0) band of its fluorescence spectrum, and the remaining symbols are defined above. As the polarity of the solvent decreases, the ability of the medium to solvate the ions decreases. The true values of ΔG_{cs} and ΔG_{cr} in a medium of arbitrary polarity can be given as

$$\Delta G_{cs} = E_{ox} - E_{red} - E_s + \Delta G_d \qquad (5)$$

$$\Delta G_{cr} = E_{red} - E_{ox} - \Delta G_d \qquad (6)$$

where ΔG_d is the energy by which the ion-pair is destabilized, when it is taken from a medium with high ϵ_s to one in which ϵ_s is low.

Using the Born dielectric continuum model of the solvent, Weller[32] derived eq 7 to calculate the ion-pair destabilization energy, ΔG_d, in a solvent with an arbitrary value of ϵ_s, if the redox potentials of the donor and acceptor are measured in a reference solvent with a high static dielectric constant, ϵ_s':

$$\Delta G_d = \frac{e_o^2}{\epsilon_s}\left(\frac{1}{2r_1} + \frac{1}{2r_2} - \frac{1}{r_{12}}\right) - \frac{e_o^2}{\epsilon_s'}\left(\frac{1}{2r_1} + \frac{1}{2r_2}\right) \qquad (7)$$

where the parameters are defined above. Thus, both λ_s and ΔG in the FCWD term, eq 2, depend on donor–acceptor distance. Therefore, it is important to compare molecules in which the donor-acceptor distances do not vary with changes in orientation.

Using E_s = 2.14 eV, E_{ox} = 0.68 V, and r_1 = 5 Å for the zinc porphyrin, E_{red} = –0.50 V and r_2 = 3.5 Å for the quinone, and the center-to-center values of r_{12} given earlier, eqs 5–7 are used to calculate ΔG_{cs} and ΔG_{cr}, the free energies for charge separation and recombination, respectively, while eq 3 is used to calculate λ_s. These data along with the FCWD term calculated from eq 2 using ω = 1500 cm^{-1} are listed in Table 2.

The data in Table 2 indicate that electron transfer from the lowest excited singlet state of the porphyrin to the quinone is thermodynamically favorable in the three solvents studied here. As the distance between the ions increases, e.g., going from SP-V to SP-H, the driving force for electron transfer in low polarity media becomes less negative because the Coulomb stabilization of the ion-pair is diminished. This effect is quite pronounced in low polarity solvents such as TOL, but it is inconsequential in higher polarity solvents, such as THF and DMF. Also, as the donor–acceptor distance increases, λ_s increases. This increase is larger for solvents in which ϵ_o and ϵ_s differ significantly. Upon examining the values of ΔG_{cs}, ΔG_{cr}, and λ_s listed in Table 2, differences in the FCWD terms alone suggest that SP-V and TD-V should have faster rates of charge separation than SP-H and TD-H, respectively. Comparing SP-V with TD-V and SP-H with TD-H shows that the rate constants for electron transfer should not depend significantly on the FCWD term. This is a simple consequence of the small difference in distance between the donor and acceptor in comparing the SP and TD spacers. Thus, any differences is observed electron transfer rate constant can be attributed directly to differences in the electronic coupling matrix element, V.

(32) Weller, A. *Z. Phys. Chem. N.F.* **1982**, *133*, 93.

Table 3. Observed (and Calculated) Rate Constant Ratios

	SP-V/TD-V		SP-H/TD-H	
	CS	CR	CS	CR
toluene	6.9 (0.8)	12.1 (1.5)	0.74 (1.4)	2.0 (1.1)
THF	8.1 (1.1)	1.3 (1.0)	3.4 (1.0)	2.0 (1.0)
DMF	1.6 (1.1)	3.2 (1.1)	2.4 (1.1)	4.4 (1.1)

The data in Table 3 compare rate constant ratios for SP-H, SP-V, TD-H, and TD-V based on the experimental data in Table 1 with those calculated from the FCWD data in Table 2. The calculated rate constant ratios assume that V is constant throughout the series. Thus, the observed differences between the experimental and calculated rate constant ratios should reflect the actual changes in V within this series of donor–acceptor molecules. The main structural difference between the molecules containing the SP spacer and those possessing the TD spacer is the 90° orientation change of the quinone. This change in donor–acceptor orientation may result in a significant change in V. In the discussion that follows three contributions to V will be considered. These contributions include a direct interaction between the donor and acceptor, V_D, an indirect interaction through the covalent bonds that connect the donor with the acceptor, V_I, and a non-covalent indirect interaction through the solvent molecules that lie between the donor and acceptor, V_{IS}. The total electronic coupling matrix element, V is the sum of these terms:

$$V = V_D + V_{IS} + V_I \qquad (8)$$

Changes in V_D can be related directly to changes in orbital overlap between the orbitals of the donor and the acceptor. Orbital overlap diminishes exponentially as the distance between the donor and acceptor increases.[33–36] Moreover, orbital overlap depends on the mutual orientation of the π systems of the donor and acceptor. Another important consideration is the interaction of the spacer orbitals with those on the electron donor and acceptor. Good evidence exists that in most covalently-linked donor–acceptor molecules quantum mechanical mixing of the spacer orbitals with those of the donor and acceptor plays a principal role in transmitting the electron from the donor to the acceptor.[37] The spatial properties and energies of the spacer orbitals, as well as their symmetries, are important in determining the degree to which they modulate the indirect interaction, V_I, between the donor and acceptor. Finally, the donor and acceptor can interact through similar mixing of the donor and acceptor orbitals with those of the solvent molecules. This contribution to the electronic coupling, V_{IS} is thought to be weaker because it involves only non-bonded interactions.[38]

It is very difficult to separate the direct interaction, V_D, between the donor and acceptor from the indirect interaction mediated by

(33) Beratan, D. N.; Hopfield, J. J. *J. Am. Chem. Soc.* **1984**, *106*, 1584.
(34) Larsson, S.; Volosov, A. *J. Chem. Phys.* **1986**, *85*, 2548.
(35) Closs, G. L.; Miller, J. *Science* **1988**, *240*, 440.
(36) Paddon-Row, M. N.; Verhoeven, J. W. *New J. Chem.* **1991**, *15*, 107.
(37) Won, Y.; Friesner, R. A. *Biochim. Biophys. Acta* **1988**, *935*, 9.
(38) Beratan, D. N.; Onuchic, J. N.; Winkler, J. R.; Gray, H. B. *Science* **1992**, *258*, 1740.

the solvent, V_{IS}, by examining covalently-linked donor–acceptor molecules in condensed media. In principle, it is possible to gauge the magnitude of V_{IS} by studies of donor–acceptor systems in which solvent molecules are positioned at fixed distances and orientations between the donor and acceptor through the use of molecular recognition strategies.[39] In addition, the magnitude of V_D can be studied by examining donor–acceptor interactions within covalently-linked donor–acceptor molecules in the gas phase.[40] Under our experimental conditions we consider the terms within the sum $V_D + V_{IS}$ to be inseparable. Nevertheless, we can examine our data for solvent dependencies of the total electronic coupling that may give some clue as to the importance of solvent-mediated electronic coupling.

In toluene the rate constant ratios SP-V/TD-V are large for both CS and CR, and far exceeded those predicted by consideration of the FCWD term alone. However, when the acceptor is positioned further away from the donor, the rate constant ratios SP-H/TD-H for both CS and CR are comparable to those predicted by the FCWD term. If we assume that the indirect interaction, V_I, through the SP and TD spacers for both the -H and -V orientations is similar, the rate constant ratios suggest that $V_D + V_{IS}$ is larger for the SP-V and TD-V molecules than for the corresponding SP-H and TD-H molecules, respectively. The effectiveness of hole and electron transmission through the SP and TD spacers will be discussed below. The relative rate ratios for the CR reactions in toluene exhibit characteristics similar to those observed for the CS reaction. This occurs despite the fact that the CS and CR reactions are expected to have different values of V because the initial and final states of the CS and CR reactions are different. Rotation of the quinone from the orientation enforced by the SP spacer to that enforced by the TD spacer greatly decreases the rate of ion-pair recombination in the -V molecules. This effect is again diminished at the longer donor–acceptor distances in the -H molecules.

Data for the CS reaction obtained in THF exhibit a large rate constant ratio SP-V/TD-V, while SP-H/TD-H is again smaller. Nevertheless, SP-H/TD-H remains about three times larger than that predicted by consideration of the FCWD term alone. The corresponding rate constant ratios for the CR reaction are smaller than those for CS. Once again, given the assumption of constant V_I, the rate constant ratios support the idea that the observed orientation dependence for the -V molecules, which possess the closer donor–acceptor distance, is an indication of the dominance of the $V_D + V_{IS}$ term.

In DMF the CS reaction displays only a small orientation dependence at both donor–acceptor distances examined. On the other hand, the orientation dependence of the CR reaction produces rate constant ratios of 3–4. These data taken in the context of the data obtained in the other two solvents suggest that the orientation effects that we observe may depend on solvent polarity in ways that are more subtle than suggested by eqs 3–7. Comparisons of rate constant ratios between the ~9 Å distance of the -V molecules with the corresponding data for the ~12 Å distance of the -H molecules suggest that the overall rates are faster at closer distances. This may be caused by changes in the V_{IS} contribution to V.

The assumption that V_I is constant throughout this series of spacer molecules can be examined more closely. The V_I term can be estimated by calculating the electronic interaction of π orbitals across the SP and TD spacers. Paddon-Row and Jordan have presented extensive photoelectron spectroscopic data and molecular orbital calculations which suggest that an estimate of the interaction energy between two double bonds separated by a hydrocarbon spacer based on Koopmans' theorem can be used to give a reasonable estimate of the electronic coupling matrix element.[41,42] Curtiss et al. have performed MO calculations using the natural bond order approach to factor the total interaction into separate contributions between specific bonds.[43] For our purposes we wish to derive an estimate of the total interaction across the spacer, irrespective of which specific bonds are involved. To this end we used the AM1 semiempirical molecular orbital treatment of calculate the energies of the two highest occupied MOs and the two lowest unoccupied MOs of the SP-diene and TD-diene illustrated below.[44] The energy difference between the pair of HOMOs, ΔE_π, on SP can be compared with that of TD to estimate V for hole transfer, while the corresponding energy difference between the pair of LUMOs, ΔE_{π^*}, for SP can be compared with that of TD to estimate V for electron transfer. The calculated energies are given in Table 4. The calculated data for the TD spacer suggest that it is substantially more effective for the transmission of holes than is the SP spacer, while the SP spacer is only slightly favored for electron transfer.

Table 4. Molecular Orbital Energies Calculated by AM1 on SP and TD Dienes (eV)

	SP		TD	
orbital	energy	splitting	energy	splitting
LUMO+1	1.373641	$\Delta E_{\pi^*} = 0.042073$	1.340366	$\Delta E_{\pi^*} = 0.034007$
LUMO	1.331568		1.306359	
HOMO	-9.494864	$\Delta E_\pi = 0.001838$	-9.486744	$\Delta E_\pi = 0.102793$
HOMO-1	-9.496702		-9.589537	

SP-diene TD-diene

In the molecules discussed here the CS reaction is an electron transfer. As such, the results of the MO calculations on the SP-diene and TD-diene predict the V_I for the SP and TD spacers in these molecules should be similar. The difference in position of attachment of the porphyrin to the spacer should account for no better than a factor of two in favor of the -V molecules. These calculations support our original assumption of approximately constant V_I, and our interpretation that the rate ratio data for CS support a dominant $V_D + V_{IS}$ term. On the other hand, the CR reaction can be either an electron or a hole transfer. If electron transfer is the mechanism of charge recombination, arguments analogous to those given above for the CS reaction can be applied to the CR reaction. However, if the CR reaction is a hole transfer, the MO calculations predict that V_I for hole transfer should be about 50 times larger for the TD spacer than for the SP spacer. Our data show that the rate constant ratios SP-V/TD-V and SP-H/TD-H for the charge recombination reactions are all >1. This suggests that either variations in V_I between the SP and TD spacers due to a contribution from hole recombination must be small, or the $V_D + V_{IS}$ term for the SP spacer must be much greater than 50 times the V_I term when compared to the same terms in the molecules using the TD spacer. We favor the interpretation that electron transfer is responsible for the CR reaction with the result that V_I is comparable for SP and TD.

The similarity of the V_I terms for the SP and TD spacers lends further support to the idea that the rate constants for both the CS and CR reactions are dominated by the $V_D + V_{IS}$ term. However, as mentioned above, unusual solvent effects may influence the observed rate constants. These may be considered

(39) Sessler, J. L.; Wang, B.; Harriman, A. *J. Am. Chem. Soc.* **1993**, *115*, 10418.
(40) Shou, H.; Alfano, J. C.; Van Dantzig, N. A.; Levy, D. H.; Yang, N. C. *J. Chem. Phys.* **1991**, *95*, 711.
(41) Paddon-Row, M. N. *Acc. Chem. Res.* **1994**, *27*, 18.
(42) Shephard, M. J.; Paddon-Row, M. N.; Jordan, K. D. *Chem. Phys.* **1993**, *176*, 289.
(43) Curtiss, L. A.; Naleway, C. A.; Miller, J. R. *Chem. Phys.* **1993**, *176*, 387.
(44) Dewar, M. J. S.; Zoebisch, E. G.; Healy, E. F.; Stewart, J. J. P. *J. Am. Chem. Soc.* **1985**, *107*, 3902.

a manifestation of the V_{IS} term. In toluene, which possesses a π symmetric high-lying HOMO and low-lying LUMO, one might expect that the mixing of these orbitals with those of the π system of the donor and acceptor would be favorable on both symmetry and energetic grounds. Unusual stabilization of ion pairs has been observed previously in toluene and benzene.[14] However, this does not explain why the CS rate constant ratio SP-V/TD-V remains high in THF, and diminishes further in DMF. Moreover, it does not explain why the rate constant ratio for the CR reaction increases in going from THF to DMF.

At least one THF or DMF is most likely coordinated to the Zn within the porphyrin in its ground electronic state, so that at least one solvent molecule that lies between the donor and acceptor possesses a restricted configuration relative to the donor and acceptor. However, after formation of the ion-pair state, the porphyrin–quinone molecules possess a large dipole moment with a large resultant electric field that could serve to selectively align dipolar solvent molecules between the donor and acceptor. The electric field will depend on the orientation of the donor relative to the acceptor. In addition, the degree to which dipolar solvent molecules orient in the electric field produced by the ion-pair state will depend the strength of the solvent dipole. Thus, it is reasonable that the sensitivity of the CR reaction to the dipole moment of the solvent may be coupled to a sensitivity to donor–acceptor orientation.

The picture that our data presents is one of subtle complexity underlying electronic coupling between a donor and acceptor despite the significant control of donor–acceptor orientation achieved in these molecules. The orientation dependent contributions of the different terms to the total electronic coupling between the donor and acceptor begin to be discernible in these molecules. Further refinements of structure in molecules of this type will be necessary to completely separate these terms. In addition, further work on non-covalent interactions between solvent molecules and donor–acceptor molecules is needed to fully understand these phenomena.

Acknowledgment. Work at ANL was supported by the Division of Chemical Sciences, Office of Basic Energy Sciences, U.S. Department of Energy under contract W-31-109-Eng-38.